JOURNAL OF MATERIALS SCIENCE 18 (1983) 3377–3386

Some electrical properties of amorphous thin films of mixed SiO and TiO

M. ILYAS, C. A. HOGARTH
Department of Physics, Brunel University, Uxbridge, Middlesex, UK

Electrical conduction in Cu–SiO/TiO–Cu thin film structures has been investigated. Prior to electroforming, the d.c. conduction showed a behaviour of the form $\log I_c \propto (V_b)^{1/2}$ where I_c is the circulating current and V_b is the applied voltage. At low applied voltages the a.c. conductivity obeyed the relation $\sigma_{AC} \propto f^n$ ($n = 0.82$ at 209 K). After electroforming, the samples showed voltage controlled negative resistance (VCNR), electron emission and voltage memory effects which can be explained in terms of a filamentary model.

1. Introduction

In amorphous solids the d.c. conductivity, I_c at a high applied field E is often found to obey the relation

$$I_c \propto \exp\left(\frac{\beta_{PF}E^{1/2} - \phi}{kT}\right)$$

where β_{PF} the Poole–Frenkel constant is given by $(e^3/\pi\epsilon_0\epsilon_R)^{1/2}$ in which e is the electronic charge, ϵ_R is the high frequency dielectric constant and ϕ is the energy of localized donors below the insulator conduction band. Work of Jonscher and Ansari [1], Hartman *et al.* [2], Hirose and Wada [3], Stuart [4] and Deery *et al.* [5] confirmed that electrical conduction in insulating films of silicon oxide is bulk limited. The experimental values of β_{PF} worked out by them lie in the range $1.38 \sim 2.6 \times 10^{-5}\,\text{eV}\,\text{m}^{1/2}\,\text{V}^{-1/2}$, whereas taking a theoretical value for ϵ of 4 gives $\beta_{PF} = 3.8 \times 10^{-5}\,\text{eV}\,\text{m}^{1/2}\,\text{V}^{-1/2}$.

Pollack and Geballe [6] have shown that for hopping processes, the a.c. conductivity σ_{AC} at low frequency f obeys the law $\sigma_{AC} \propto f^n$ where n takes the value between 0.5 and 1.0 depending on temperature. Argall and Jonscher [7] showed that sandwich films of SiO_x and Al_2O_3 exhibit this type of behaviour at low frequencies.

It is now well known that many insulators in the form of oxides [8–12], halides [13], sulphides [14, 15] and polymer [16, 17] type of materials sandwiched between metal electrodes undergo electroforming at a certain voltage V_F followed by voltage-controlled negative resistance (VCNR), electron emission, electroluminescence and memory effects. Various models have been proposed by Hickmott [8, 9], Simmons and Verderber [10], Greene *et al.* [13], Dearnaley *et al.* [18] and Ralph and Woodcock [19] to explain electroforming and associated characteristics, although none is entirely satisfactory. The filamentary model proposed by Dearnaley *et al.* [18] together with some modifications seems to be most appropriate according to which current in formed insulating layers is carried by filaments bridging the two electrodes, and a band structure is associated with each filament. In this paper, conduction before and after electroforming in Cu–SiO/TiO–Cu, previously studied by Bidadi and Hogarth [20], with thickness of insulator up to 1300 nm is reported. After electroforming we observed VCNR, electron emission and a voltage-memory effect. Voltage–temperature-memory and pressure–voltage-memory effects in this system have been reported previously [21].

2. Experimental details

Films were evaporated by a technique of thermal evaporation in a Balzers 510 coating unit on to clean Corning 7059 glass substrates as previously described [22]. D.C. electrical measurements were made by the conventional method in a subsidiary vacuum system equipped with the necessary

0022–2461/83 $03.00 + .12 © *1983 Chapman and Hall Ltd.*

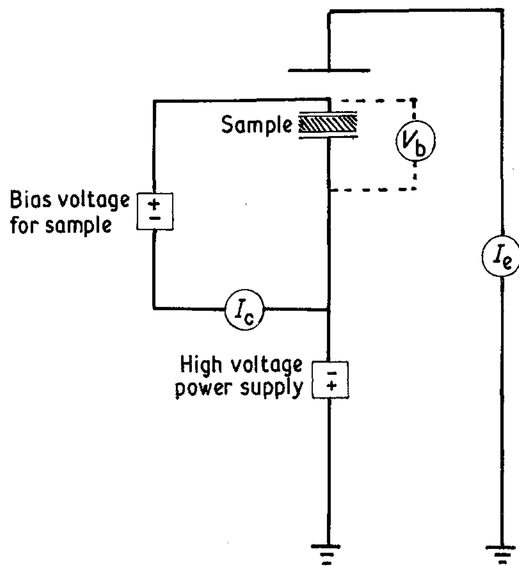

Figure 1 Circuit diagram for measuring circulating (I_c) and emission (I_e) currents for different values of applied voltage (V_b).

facilities. The electrical circuit for measuring the voltage–current characteristics is shown in Fig. 1. A d.c. bias voltage was supplied by a Coutant/Solartron power supply and the circulating current was measured by an electronic avometer or an electrometer, depending on the level of current in the circuit. The emitted electrons were collected by a copper plate 8 cm x 3 cm placed at a distance of 2 cm from the top electrode and with the base electrode negatively biased at 100 V by a Keithley high voltage regulated power supply, and were measured by using another electrometer. A.C. measurements were made by using a Wayne Kerr universal bridge B221 along with a Wayne Kerr audio-frequency voltage generator S121 as source and a Wayne Kerr wave form analyser A321 as detector. A block diagram for the experimental arrangement is shown in Fig. 2.

3. Results and discussion

3.1. Conduction mechanism prior to electroforming

Voltage–current characteristics for a Cu–SiO/TiO–Cu device 680 nm thick are shown in Fig. 3. An ohmic region for bias voltage $V_b < 1$ V is followed by a non-ohmic region in which the circulating current I_c is a monotonically increasing function of V_b. I_c increases suddenly at $V_b \simeq 3$ V indicating the onset of electroforming as shown by curve (a). To study the characteristics before electroforming, the value of V_b was kept less than 3 V. Fig. 4 shows the graphs of $\log I_c$ against $(V_b)^{1/2}$ for the same sample, resulting in a straight line in the non-ohmic region, i.e. $1 \text{ V} < V_b < 3 \text{ V}$, suggesting the conduction mechanism to be either of the Poole–Frenkel or Schottky form. The gradient of the linear portion, $m = 0.93 = (e \ln \beta)/(kTd^{1/2})$, yields an experimental value of $\beta = 4.46 \times 10^{-5} \text{ eV m}^{1/2} \text{V}^{-1/2}$. The theoretical value of $\beta_{PF} = (e^3/\pi\epsilon_R\epsilon_0)^{1/2}$ using $\epsilon_R = 6$ calculated from capacitance measurement at 20 kHz comes out to be $3.1 \times 10^{-5} \text{ eV m}^{1/2} \text{V}^{-1/2}$. The theoretical value of β_S (Schottky) is half of β_{PF}. The experimental value of β for the system under investigation lies close to β_{PF}. We may therefore regard the high-field conduction mechanism to be predominantly of the Poole–Frenkel type. Furthermore we discard the Schottky mechanism, as the experimental value of β leads to an unreasonbly small value of permittivity ϵ. Fig. 5 shows $\log I_c$ against $(V_b)^{1/2}$ curves for a thicker sample at different temperature. The slope of the linear portion of the curve at 296 K gives $\beta = 4.7 \times 10^{-5} \text{ eV m}^{1/2} \text{V}^{-1/2}$, almost the same as mentioned earlier. The activation energy ΔE estimated by using the relation $I_c = I_0 \, e^{-\Delta E/kT}$ is found to be $\simeq 0.5$ eV, a value typical of many amorphous semiconductors in which the conductivity increases with rise of temperature.

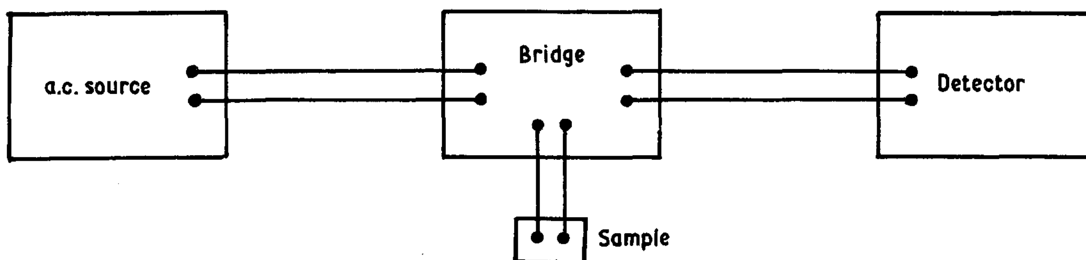

Figure 2 Schematic diagram for a.c. measurements.

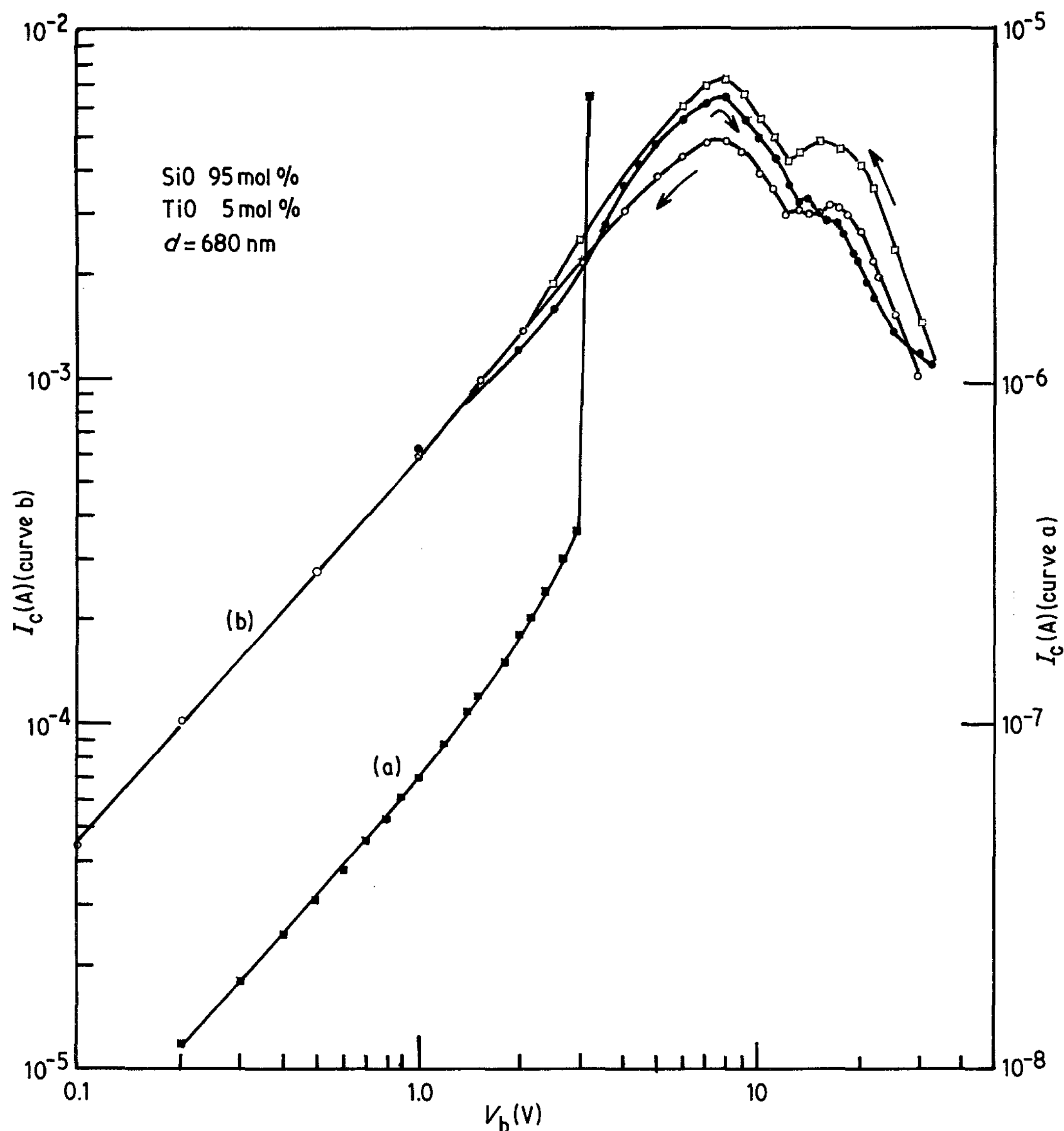

Figure 3 Voltage–current characteristics for a Cu–SiO/TiO–Cu sandwich sample (a) before forming and (b) after forming. –o– with decreasing V_b in first cycle, –•– with increasing V_b in second cycle, –□– with decreasing V_b in second cycle.

A.C. measurements were made to study the conduction mechanism in the ohmic region and the dependence of a.c. conductance on frequency f at different temperatures at 0.7 V RMS is shown in Fig. 6. A power-law relation of the form σ_{AC} = constant $\times f^n$ is obeyed for $2 \times 10^3 \text{Hz} < f \leqslant 2 \times 10^4 \text{Hz}$ and the exponent n takes the value 0.65 at 348 K and 0.82 at 209 K. The activation energy at 20 kHz $\simeq$ 0.02 eV. Fig. 7 represents the variation of capacitance with frequency and this is nearly constant. The observed low value of activation energy, a linear relation between V_b and I_c, a slight decrease of polarizability with f and the power law dependence of σ_{AC} on f are typical characteristics of a hopping conduction mechanism. We therefore regard the conduction in the ohmic region to be due to hopping processes.

3.2. Conduction after electroforming

3.2.1. Electroforming and VCNR

Electroforming was initiated at $V_b \simeq 3$ V and was performed in vacuum by increasing V_b from zero up to 25 V in steps of 1 V with some lapse of time. Samples up to a thickness of 1.3 μm could be

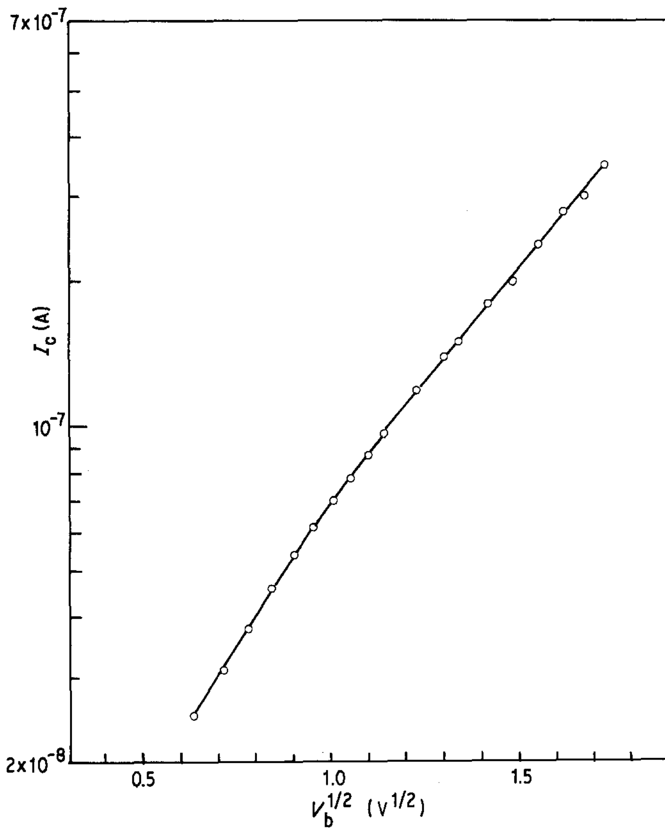

Figure 4 Dependence of $\log I_c$ on $V_b^{1/2}$ before forming for the sample of Fig. 3 ($m = 0.93$, $\epsilon_{R_{PF}} = 2.89$, $\beta = 4.46 \times 10^{-5}$ eV $m^{1/2}$ $V^{1/2}$).

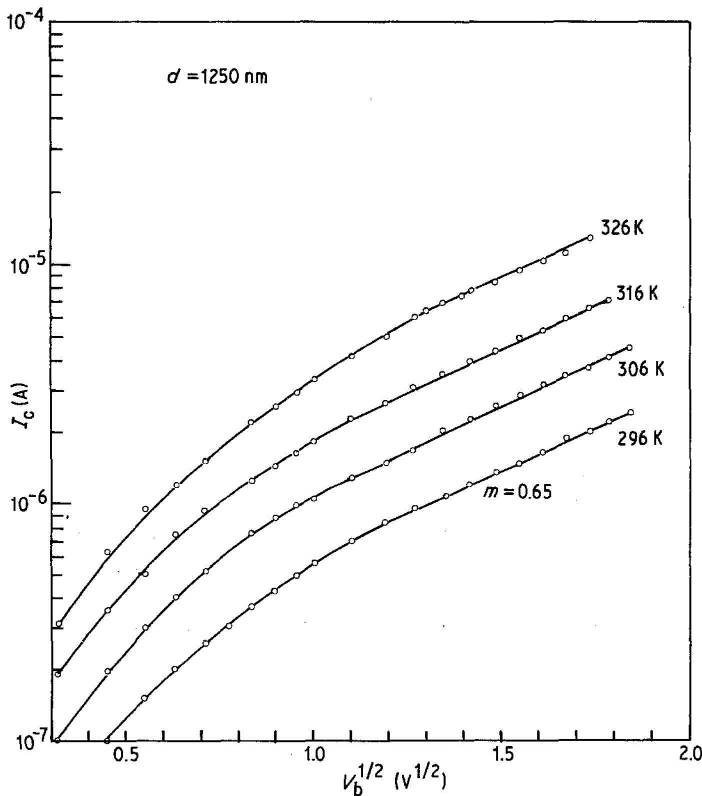

Figure 5 $\log I_c$ as a function of $V_b^{1/2}$ at several temperatures for a thicker Cu–SiO/TiO–Cu sandwich sample of composition SiO, 90 mol%; TiO, 10 mol% ($\epsilon_{R_{PF}} = 2.62$, $\beta = 4.7 \times 10^{-5}$ eV $m^{1/2}$ $V^{1/2}$).

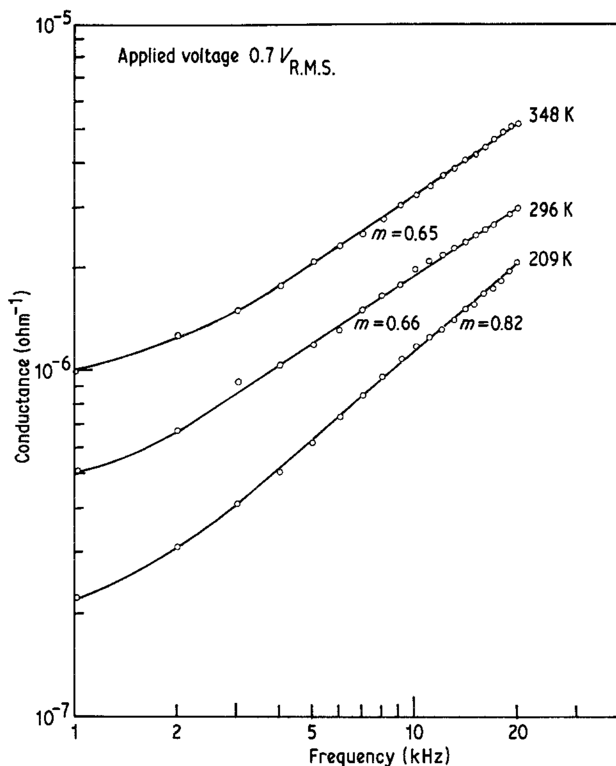

Figure 6 A.C. conductance as a function of frequency for the sample of Fig. 3.

electroformed in this way. The conduction in electroformed samples increased by about 4 orders of magnitude and showed VCNR in the $V_b - I_c$ characteristics and electron emission into vacuum. Fig. 3 and Fig. 8 show the $V_b - I_c$ characteristics for 680 and 300 nm thick electroformed samples and these are fairly reproducible for forward and reverse runs. The maximum peak current I_m corresponds to a value of V_b lying between 5 and 7 V and is higher for thinner samples and increases with increase of molar percentage of TiO. It was further observed that a change of polarity had no effect on the $V_b - I_c$ characteristics and formed samples could be deformed in air.

The results can be explained on a filamentary model of electrical conduction. During electroforming, conducting filaments made of chains of metals atoms alternating with anion vacancies develop across the insulating layer and bridge the electrodes. Conduction after electroforming takes

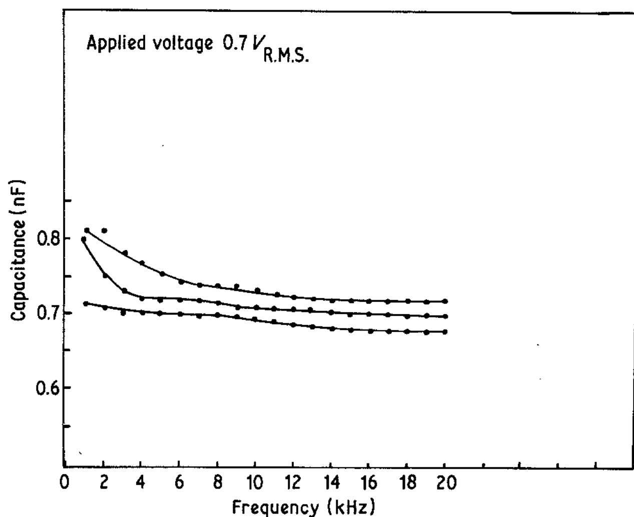

Figure 7 Dependence of capacitance on frequency for the sample of Fig. 6.

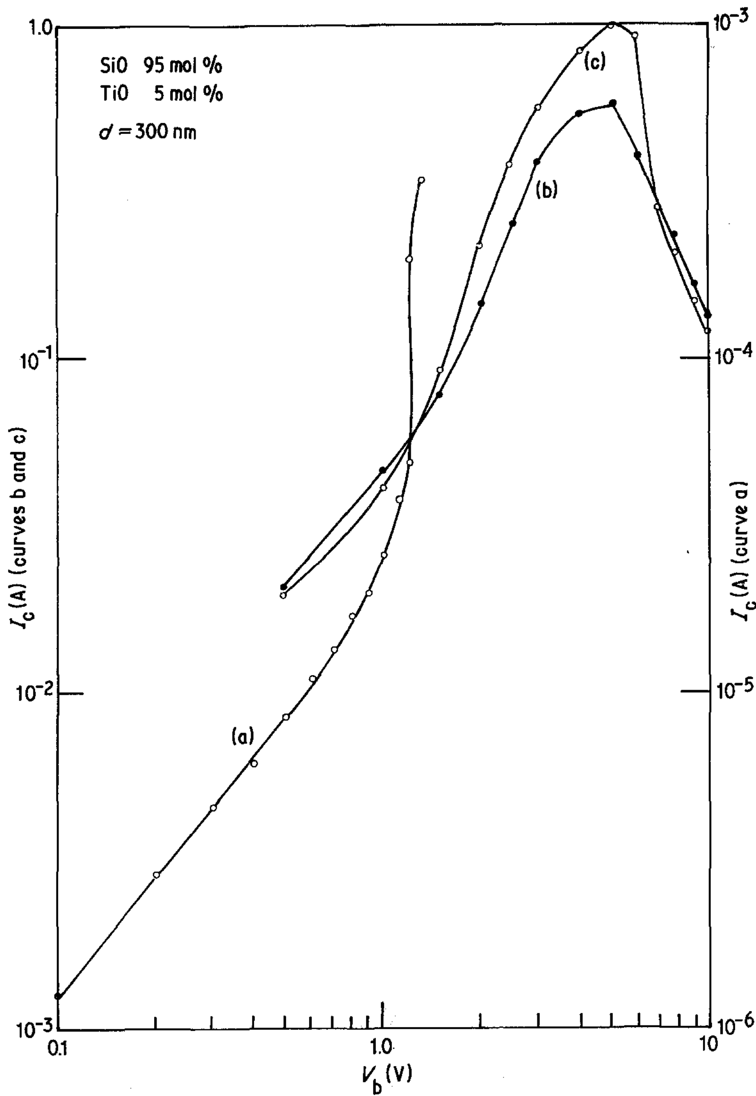

Figure 8 Voltage–current characteristics for a Cu–SiO/TiO–Cu sandwich sample (a) before forming, (b) after forming (at 293 K) and (c) after forming (at 244 K).

place with the assistance of these filaments and hence the conductivity level increases. Due to large power dissipation of order 0.7 watt cm^{-2} at I_m some of the filaments start rupturing at the weak points resulting in a decrease of I_c and in the manifestation of VCNR. The filaments can regrow by some kind of ionic migration resulting in reproducible $V_b - I_c$ characteristics with increasing and decreasing voltage. Before the onset of the negative resistance region, conduction by the filaments is by no means ohmic and indeed seems more likely to be due to space-charge-limited processes. It is of ohmic form for low applied voltage.

3.2.2. Electron emission

Emission current I_e and its variation with V_b for 680 and 1250 nm thick electroformed films is shown in Figs. 9 and 10, respectively. I_e starts at about 4 V (work function of Cu = 4.5 eV0 and increases with V_b. The initial noisy behaviour of I_e becomes stable in the voltage range between 15 and 30 V. A maximum value of I_e of order 0.2×10^{-5} A was observed for the active area of anode of 0.07 cm^2 and gave a fairly high value of current density of the order of 2.8 $\mu A\, cm^{-2}$. The electron emission may be attributed to a weak high resistance region of filaments near the anode. Under high fields electrons are excited to hot electron conditions, escape from the filaments, enter the anode region and are emitted. There is evidence that damage to the top electrode also assists in the emission of electrodes through regions which have been thinned down or have peeled off [20].

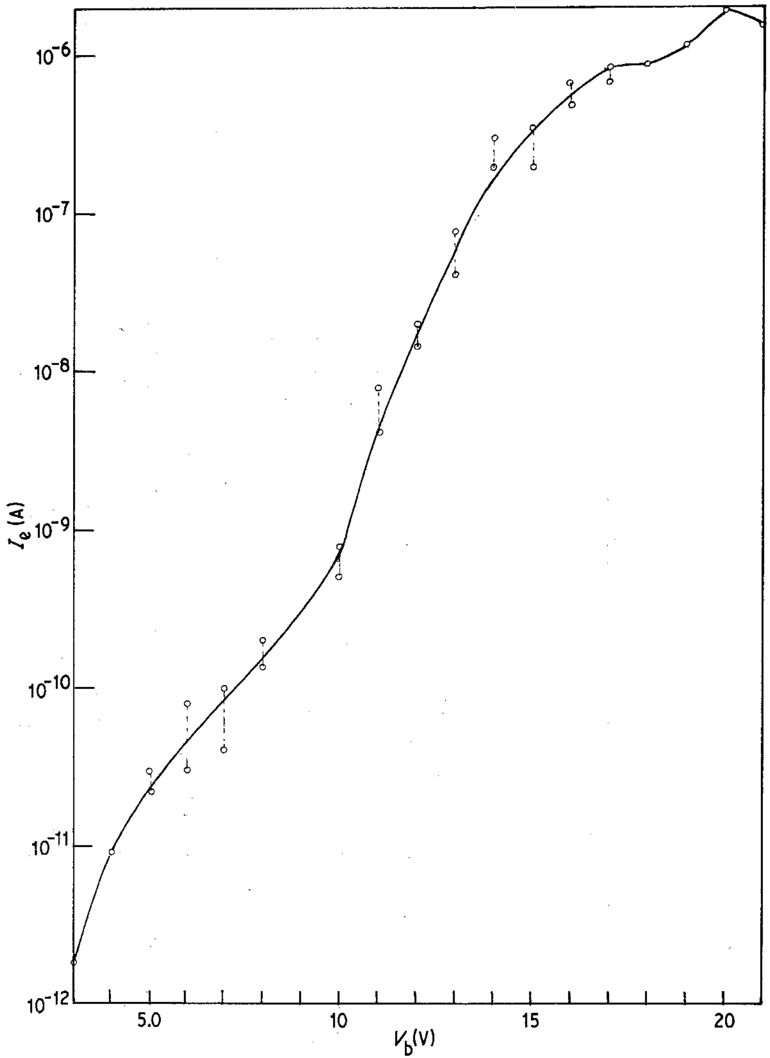

Figure 9 Emission current as a function of applied voltage for the sample of Fig. 3 after forming.

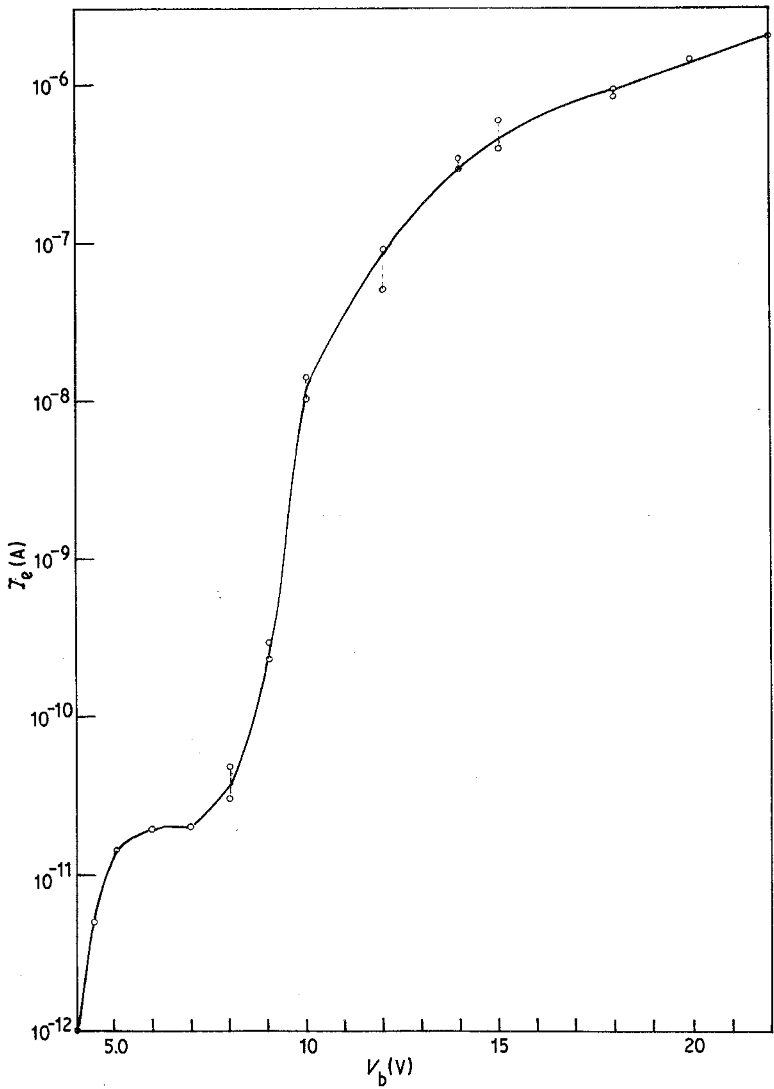

Figure 10 Emission current as a function of applied voltages for the sample of Fig. 5 after forming.

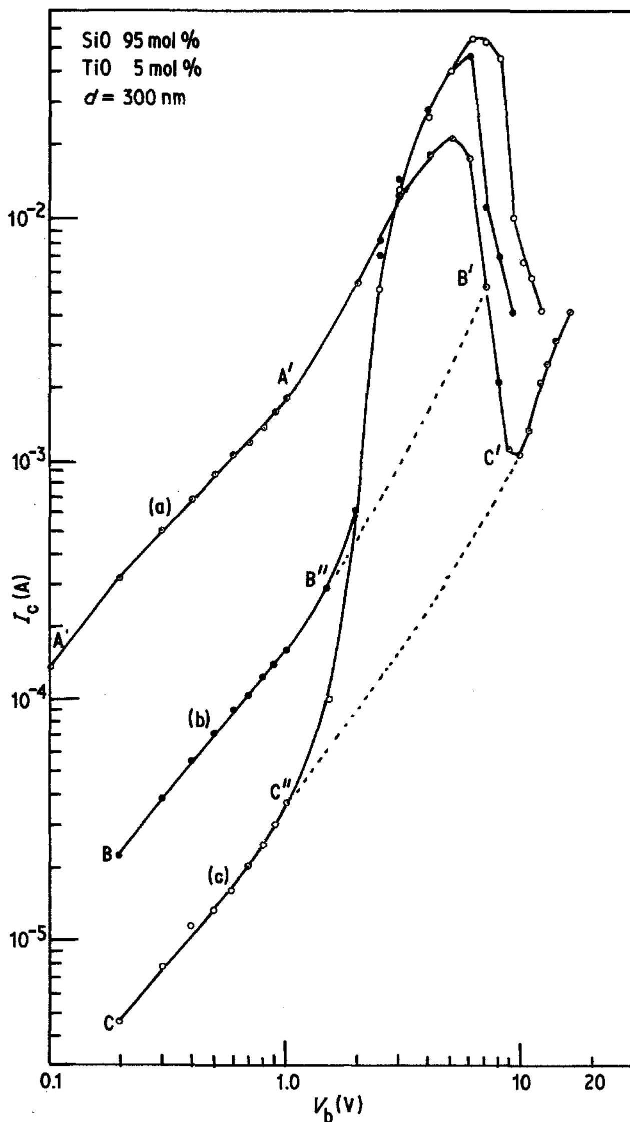

Figure 11 Voltage–current characteristics of an electroformed Cu–SiO/TiO–Cu sandwich sample showing memory states: (a) initial characteristics, (b) memory state induced at B′ (7 V) and (c) memory state induced at C′ (10 V).

3.2.3. Voltage-memory

Fig. 11 shows the voltage-memory effects of a 300 nm thick sample. Curve (a) (AA′B′C′) represents the V_b–I_c characteristics of an electroformed device. The voltage at point B′ ($V_b = 8$ V) in the negative resistance region was removed and quickly re-applied. The new V_b–I_c characteristics are shown by curve (b). The system switches to the high-impedance state BB′ and remains in this state for $V_b < 1.8$ V. Above 1.8 V the system again reverts to the low-impedance state, followed by the occurrence of negative resistance. Extrapolation of the high impedance path BB″ gives the switch-off voltage 8 V. Another memory state CC″ could also be obtained by removing V_b at C′ (10 V) and re-applying it quickly. In the latter case the device switches to a high impedance state. Applying a voltage greater than the threshold voltage, $V_{th} = 1.8$ V, switches the device again to its original low-impedance state. Fig. 12 shows the effects of temperature on memory states induced at 10 V. Low temperatures have little effect for $V_b < V_{th}$. Increasing the temperature above room temperature decreases V_{th}.

Voltage-memory effects are explained by Simmons and Verderber [10] in terms of trapping and release of charges within insulating films, whereas Ralph and Woodcock propose that in the memory states some of the filaments retain sufficient trapped charge to be in the high-impedance state. The erasing of a memory state is due to detrapping (field emission) of stored charges by

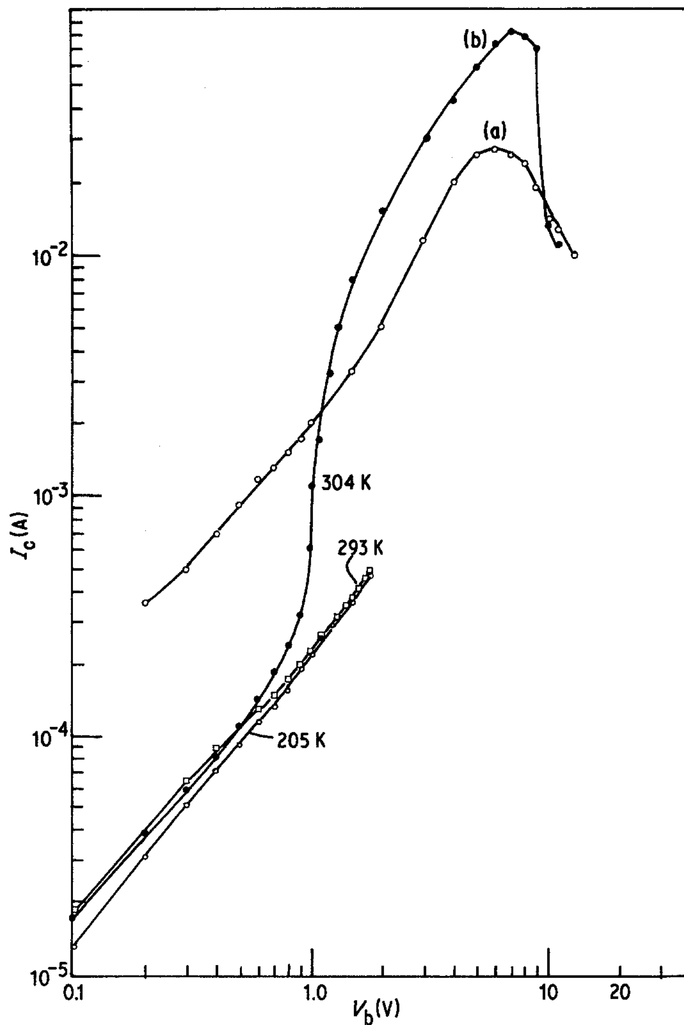

Figure 12 Voltage–current characterstics for the same sample as in Fig. 11 showing the effects of temperature on V_{th}, the memory state induced at 10 V at 293 K: (a) initial characteristics at 293 K and (b) characteristics at 304 K.

filaments and is dependent on the field distribution inside and around the high resistance filaments. The field inside the filaments appears across a narrow region of trapped charges resulting in a local high field. When this field reaches a sufficient level the electrons trapped in localized levels will be rapidly released. The charges in the traps outside the filaments relax into traps inside the filaments. The threshold voltage is that voltage across a filament constriction at which field emission of trapped charges into the conduction band takes place. Below V_{th} the conduction is mainly due to trapped charges. V_{th} is dependent on temperature as a rise in temperature of sample assists in field emission from the traps.

Acknowledgement

One of us (MI) would like to thank the Government of Pakistan for awarding a C.O.T. Scholarship for higher studies.

References

1. A. K. JONSCHER and A. A. ANSARI, *Phil. Mag.* **23** (1971) 205.
2. T. E. HARTMAN, J. G. BLAIR and R. BAUER, *J. Appl. Phys.* **37** (1966) 2468.
3. H. HIROSE and Y. WADA, *Jpn. J. Appl. Phys.* **3** (1964) 179.
4. M. STUART, *Brit. J. Appl. Phys.* **18** (1967) 1637.
5. M. DEERY, J. G. PERKINS and K. G. STEPHENS, *Thin Solid Films* **8** (1971) R16.
6. M. POLLACK and T. G. GEBALLE, *Phys. Rev.* **122** (1961) 1742.
7. F. ARGALL and A. K. JONSCHER, *Thin Solid Films* **2** (1968) 185.
8. T. W. HICKMOTT, *J. Appl. Phys.* **33** (1962) 2669.
9. *Idem, ibid.* **35** (1964) 2118.
10. J. G. SIMMONS and R. R. VERDERBER, *Proc. R. Soc. A.* **301** (1967) 77.
11. R. A. COLLINS and R. D. GOULD, *Solid State Electron.* **14** (1971) 805.
12. R. D. GOULD and C. A. HOGARTH, *Int. J. Electron.* **37** (1974) 157.
13. P. D. GREENE, E. L. BUSH and I. R. RAWLINGS,

Proceedings of the Symposium Deposited Thin Film Dielectric Materials, Montreal, 1968, edited by F. Vratny (Electro-Chemical Society, New York, 1969) p. 167.
14. R. R. SUTHERLAND, *J. Phys. D.* **4** (1971) 468.
15. R. R. SUTHERLAND, J. P. A. WILLIAMSON and R. A. COLLINS, *ibid.* **5** (1972) 1686.
16. H. T. MANN, *J. Appl. Phys.* **35** (1964) 2173.
17. K. H. GUNDLACH and J. KADLEC, *Phys. Status Solidi (a)* **10** (1972) 371.
18. G. DEARNALEY, D. V. MORGAN and A. M. STONEHAN, *J. Non-cryst. Solids* **4** (1970) 593.
19. J. E. RALPH and J. M. WOODCOCK, *ibid.* **7** (1972) 236.
20. H. BIDADI and C. A. HOGARTH, *Thin Solid Films* **27** (1975) 319.
21. C. A. HOGARTH and M. ILYAS, *ibid.* **103** (1983) 267.
22. C. A. HOGARTH and L. A. WRIGHT, Proceedings of the International Conference on Physical Semiconductors, Moscow, July 1968 (Nauka, Leningrad, 1968) p. 1274.

Received 11 March
and accepted 18 March 1983